IOSR Journal of Applied Physics (IOSR-JAP)
e-ISSN: 2278-4861.Volume 8, Issue 6 Ver. III (Nov. - Dec. 2016), PP 154-158
www.iosrjournals.org

Magnetic and Magnetoelectric Properties of ZnMnGeAs Alloy Films

Yunki Kim[1], J. B. Ketterson[2]
[1](*Department of Electrical and Biological Physics, Kwangwoon University, Seoul 01897, Republic of Korea)*
[2](*Department of Physics & Astronomy, Northwestern University, Evanston, IL 60208, USA)*

Abstract: *Thin alloy films of ZnMnGeAs were grown on Si substrates. Magnetization and resistance measurements were used to show that the ZnMnGeAs film samples have magnetic transitions above room-temperature. From hysteresis in magnetic field dependent magnetization measurements, the transitions were confirmed to be a ferromagnetic phase transitions. Magnetoresistance (MR) was measured in the deposited films, showing negative and positive MR effects depending on the temperature. The Hall measurements showed that ZnMnGeAs films have n-type carriers.*

Keywords: *ZnMnGeAs, room-temperature ferromagnetism, diluted magnetic semiconductors, thin films*

I. Introduction

In recent decades, II-IV-V_2 chalcopyrites have attracted much attention for application involving nonlinear optical devices, solar cells, and detectors due to the anisotropy caused by their chalcopyrite orderings and structural similarity to the popularly used tetrahedrally-coordinated III-V zinc-blende semiconductor materials [1]. Though they are nonmagnetic, the chalcopyrites (II-IV-V_2) doped with magnetically active impurities such as Mn have been reported to show ferromagnetic (FM) behaviors near room temperature [2,3]. Pure elemental group IV semiconductors such as Ge are intrinsically nonmagnetic, as are other known semiconductor materials. However, semiconductor Ge highly doped with Mn has been revealed to display ferromagnetic ordering near room temperature (around 270 K), as reported for a GeMn alloy sample with 6% Mn composition [4]. The chalcopyrites and/or elemental semiconducting materials with high ferromagnetic transition temperatures can be potentially used to advance spintronic devices, by replacing the currently used ferro/antiferro-magnetic metals with semiconductors.

By using semiconductors as major elements in spintronic devices, maturely developed processing techniques in semiconductor industry as well as versatile charged carrier controllability of semiconductor devices can be merged into the spin dependent devices such as magnetoresistive (MR) sensor and magnetic tunnel junction [5] to reduce the size and enhance the performance. However, there would be large and rapid loss in spin polarization during the spin injection between nonmagnetic semiconductors and ferromagnetic metals in spintronic devices where spin polarized carrier transport is essential if we are to flow spin polarized current through the semiconductor elements from ferro/antiferro-magnetic metals [6,7]. The appearance of ferromagnetic semiconductors will solve this issue. Using ferromagnetic semiconductors lattice and Fermi-level matched with nonmagnetic semiconductors will reduce the spin-flip scattering rate at the interface.

Magnetic semiconductors prepared by substituting magnetic ions such as Mn^{2+}, Co^{2+}, Cr^{2+}, Fe^{2+}, and Ni^{2+} into non-magnetic host semiconductors are called dilute magnetic semiconductors (DMS) [8,9]. In various classes of DMS, including III-V [10,11], II-VI [12], and IV [4,13], ferromagnetism has been observed. One critical drawback of DMS is low solubility of magnetic ions in the host semiconductors which limits magnetic moments and ferromagnetic transition temperatures.

Here we report the growth of ZnMnGeAs films on Si(100) and Si(111) substrates, which can be analyzed as alloy films of $Zn_{1-x}Mn_xGeAs_2$ of chalcopyrite structure and Ge of diamond structure, and which show room-temperature ferromagnetism. The magnetic and electrical transport properties of the films will be presented. In these diluted magnetic semiconducting films, Ge rich ones with lower Mn composition show semiconducting behavior while Mn rich ones display rather metallic behavior in resistance.

II. Experiment

Thin films of $Zn_xMn_yGeAs_z$ were deposited on Si(111) and Si(100) substrates with a molecular beam epitaxy (MBE) system. Native oxide at the surface of silicon substrates was etched in hydrofluoric acid (50:1 HF) and rinsed in methanol. A nitrogen gun was used to blow and dry out any residual chemicals on the surface of the substrates, followed by heating upto 600-650 °C in a load-lock vacuum chamber to remove adsorbed unwanted molecules on the surface. The deposition rate was maintained to be around 0.5 Å/s. The substrate temperature during the growth was 600-700 °C. To monitor crystal orientation and growth mode of the growing films during the deposition, reflection high-energy electron diffraction (RHEED) was used. RHEED patterns

during the film deposition were observed. Streaky patterns were seen from the film sample grown on Si(111) at substrate temperature of 700 °C, as shown in Fig. 1 while those from the films grown at low temperatures were streaky at first then became weaker.

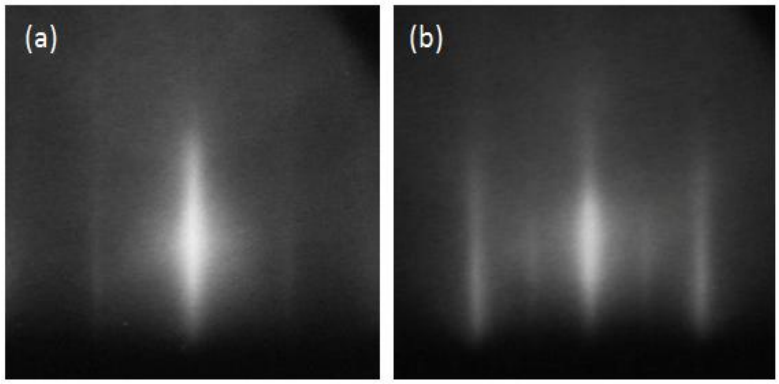

Fig. 1 RHEED images of a Mn_xGeAs_y film on Si(111) during the deposition.

III. Results And Discussions

The lattice constants for $ZnGeAs_2$ are a = 5.670 Å and c = 11.15 Å, and that for Ge is a = 5.657 Å, while those for $MnGeAs_2$ are a = 5.782 Å and c = 11.323 Å in bulk [14]. The lattice mismatches between $ZnGeAs_2$ and Si (a = 5.4307 Å), and between $MnGeAs_2$ and Si are 4.406% (2.657% with c/2) and 6.469% (4.250% with c/2); hence for our thin ZnMnGeAs layers, we could expect that the film peaks in x-ray θ-2θ diffraction (XRD) measurements would shift to lower values due to the lattice expansion along the growth direction, which was confirmed in a measured XRD $ZnGeAs_2$ film peak at 27.19° lower shifted from the bulk value at 27.377° of $ZnGeAs_2$ (112). XRD measurements for $Zn_xMn_yGeAs_z$ films on Si(100) and Si(111) substrates showed several films peaks in the XRD patterns as shown in Fig.'s 2(a) and (b). The two peaks at 31.7-31.9° and 32.3-32.9° could be identified to be (200) and (004) peaks from a chalcopyrite structural ordering, and the peaks near 66.05-66.17° could be Ge (400) or a mixture of (400) and (008) from a chalcopyrite ordering. The peaks near 42.4° can be (220) of a chalcopyrite $(Zn,Mn)GeAs_2$ or MnAs (202) and (211). From scanning electron microscope (SEM) measurement, morphology of the deposited film samples was investigated. Figure 3 shows SEM images of $Zn_xMn_yGeAs_z$ films on Si(100) and Si(111). A film deposited on Si(100) at substrate temperature of 700 °C seems to have the largest and rather smooth and flat grains as shown in Fig. 3(a), while a film grown at 600 °C looks to grow in the island type growth mode as shown in Fig. 3(b). A film deposited on Si(111) at 700 °C seems to have apparent grains with large heights. Energy dispersive x-ray spectroscopy (EDS) measurements were performed on the samples grown on Si(100) and Si(111) substrates, as summarized in TABLE 1. From the EDS measurements, the composition of Zn/Mn, Ge, and As deviates from the stoichiometric value of (1: 1: 2) of a chalcopyrite structure, but rather deficient in Zn/Mn and As but abundant in Ge. Inductively coupled plasma atomic emission spectroscopy (ICP-AES) measurements were also performed on the samples, which revealed that the composition results by EDS for Mn were underestimated and those for As were overestimated. The composition of Ge in all the samples is larger than the stoichiometric value, implying that the films can be regarded as alloy films of $(Zn,Mn)GeAs_2$ and Ge. Further fine-tuning of the composition will likely be required in achieving device-quality films.

Table 1 Compositions of Mn, Ge, and As of $MnGeAs_2$ films from EDX measurements (and from ICP-AES measurements in parenthesis) with respect to substrate orientation and growth temperature.

Substrate	Growth temperature (°C)	Zn	Mn	Composition Ge	As
Si(100)	600	(0.24)	(0.41)	(1)	(0.73)
	600	0.03 (0.05)	0.11 (0.22)	1	0.30 (0.28)
	700	0.02 (0.01)	0.38 (0.64)	1	0.27 (0.36)
Si(111)	700		(0.71)	(1)	(0.65)

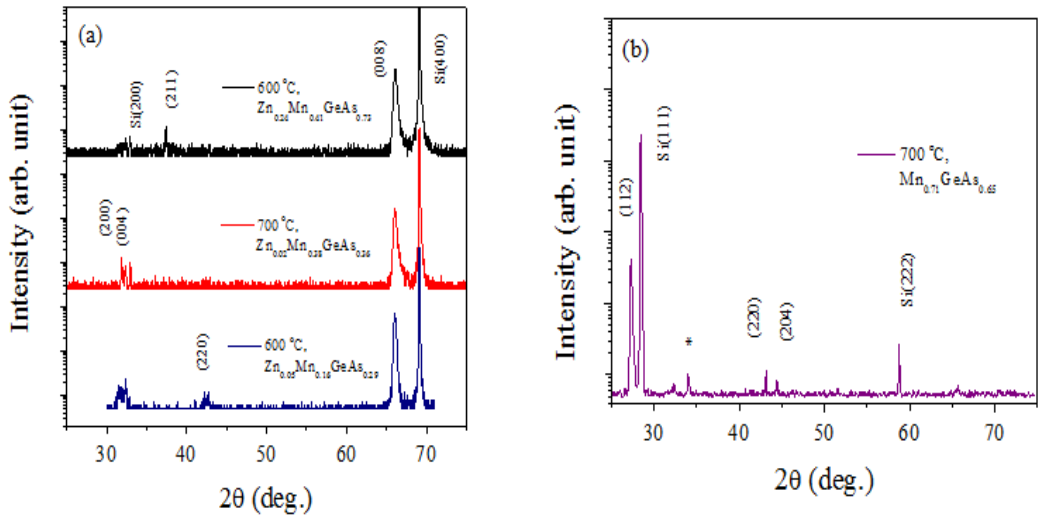

Fig. 2 *θ-2θ* XRD patterns (a) of $Zn_{1-x}Mn_xGeAs_y$ films on Si(100) substrate, deposited at substrate temperature of 600-700 ^oC, and (b) of a Mn_xGeAs_y films on Si(111) substrate deposited at 700 ^oC, on a logarithmic scale. (A peak denoted by * could not be identified with one from a chalcopyrite structure.)

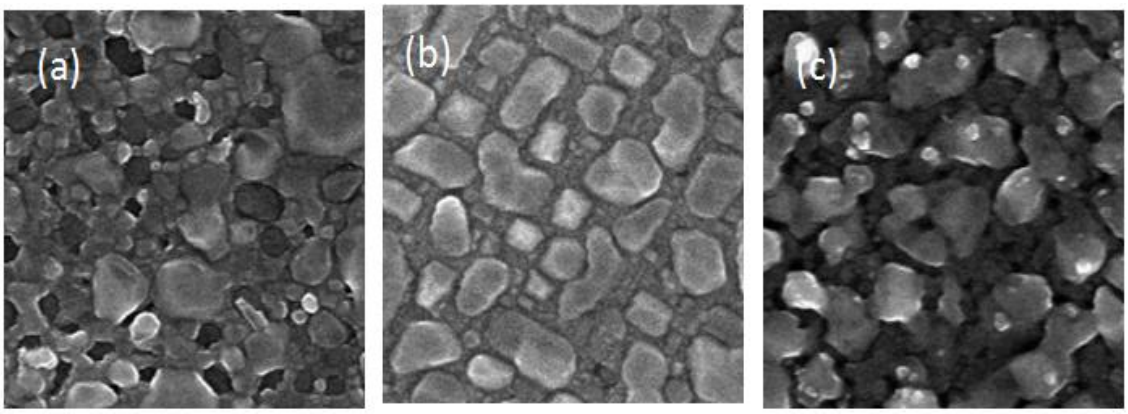

Fig. 3 SEM images of ZnMnGeAs alloy films on Si(100) deposited at substrate temperature of (a) 700 and (b) 600 ^oC, and (c) SEM images of a MnGeAs alloy film on Si(111) deposited at 700 ^oC.

The magnetization measurements on the ZnMnGeAs alloy films were performed using a SQUID (Quantum Design) magnetometer. The magnetizations (*M*) of the films grown under various growth conditions were measured in a 1000 Oe external magnetic field (*H*) from 5 to 400 K, as shown in Fig. 4(a). The measured samples display magnetic transitions around 320 K, above room temperature. Magnetizations with respect to the external magnetic field were also collected for the ZnMnGeAs alloy film samples at 5 and 300 K. Hysteresis in *M-H* curves were observed at room-temperature (300 K) and at 5 K, suggesting that the transitions around 320 K are ferromagnetic (FM)-paramagnetic (PM) transition. Temperature dependent electrical resistances of the samples are shown in the same figure, Fig. 4(a). The resistances of the films decrease with temperature up to around 320 K and then they look to saturate. The temperature where the slopes in the resistances of the film samples change matches the FM-PM transition temperature in the magnetization measurements. This can be caused by spin-flip scattering rates difference between FM and PM regions. Metallic behavior was observed from the MnGeAs alloy films as shown in Fig. 4(b), which is different from the semiconducting behavior of ZnMnGeAs alloy films. Note that the Ge contents in the ZnMnGeAs alloy film samples are larger than those in the MnGeAs alloy film and that the bandgap of $ZnGeAs_2$ is 0.85 eV while that of $MnGeAs_2$ is 0.06 eV [14]. The change in slope of the resistance curve of the MnGeAs film sample corresponds to the change in magnetization and happens at the positions near the kink at around 50 K and near the transition at around 350 K. In the MnGeAs alloy film sample, higher transition temperature was observed than the ZnMnGeAs alloy film samples. *M-H* curves for $Zn_{0.05}Mn_{0.22}GeAs_{0.28}$ film on Si(100) at growth temperature 600 ^oC are shown in Fig. 5 (a). The coercive fields of the ZnMnGeAs alloy film at 5, and 300 K are 500 and 250 Oe. The coercive fields for some of the ZnMnGeAs and MnGeAs alloy film samples are summarized in TABLE 2. At 300 K, ZnMnGeAs alloy samples show very small coercive fields.

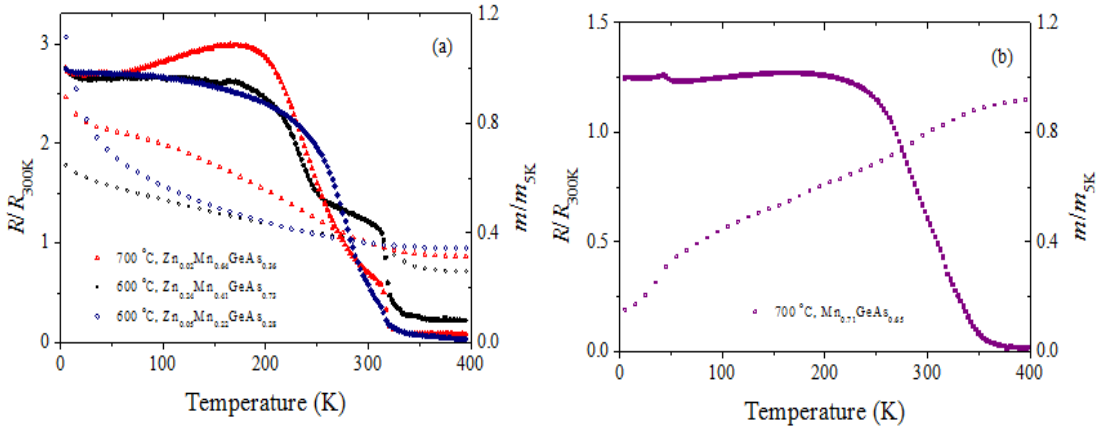

Fig. 4 (a) Temperature dependent resistance (*R*) and temperature dependent magnetization (*m*) under an external magnetic field of 1000 Oe of $Zn_{1-x}Mn_xGeAs_y$ films on Si(100) substrate, normalized by the resistance value at 300 K and the magnetization value at 5 K. (b) Resistance and magnetization curves for a $Mn_{0.71}GeAs_{0.65}$ film on Si(111) at various temperatures from 5 to 400 K.

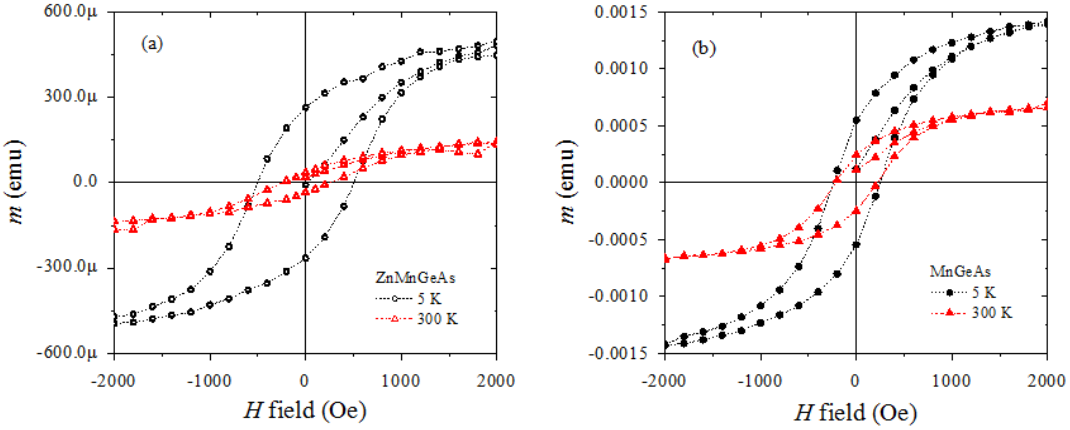

Fig. 5 (a) Field (*H*) dependent magnetization (*m*) curves of a $Zn_{1-x}Mn_xGeAs_y$ film on Si(100) at 5 and 300 K. (b) *m-H* curves for a a Mn_xGeAs_y film on Si(111) at 5 and 300 K, showing hysteric behavior.

Table 2. Coercive fields of $MnGeAs_2$ films at some temperatures (5 and 300 K for all the samples, 250 K for a film on GaAs, and 340 K for a film on Si(111)) with respect to various growth condition.

samples	Substrate	Growth temperature (°C)	Coercive Field (Oe)			
			5 K	300 K	300 K	340K
$Zn_{0.24}Mn_{0.41}GeAs_{0.73}$	Si(100)	600	200	55	40	
$Zn_{0.05}Mn_{0.22}GeAs_{0.28}$		600	500	250		
$Zn_{0.02}Mn_{0.64}GeAs_{0.36}$		700	460	65		
$Mn_{0.71}GeAs_{0.65}$	Si(111)	700	240	220		140

Magnetoresistance (MR) measurements were performed at various temperatures from 5 to 390 K in 35 K interval. The maximum MR change in fields ($R(H)/R(H=0)$ or $R(H)/R_0$) between -5 and 5 T were found not larger than 17%. The maximum negative MR, decrease down to 83% of the zero field value, was observed at 40 K and 5 T from our 35 K interval MR measurement, where aligned spins lead the decrease in resistance. As temperature increases, change in resistance decreases [15]. And at some temperature between 110 and 145 K, crossover of MR from negative to positive happened. At the temperatures above, positive MR was observed, which is caused by the increase in carrier-carrier scattering with the increasing magnetic field. The circular motion of carriers in a magnetic field increases as the magnetic field increases, which will yield a resistance increase. The increase in unpolarized carriers due to thermal excitation mostly from Ge in the MnGeAs alloy film may lead this crossover from negative to positive MR. The maximum positive MR at 5 T, 4% increase from the zero field value, was observed at 180 K in our measurement. As temperature goes up, the change in resistance with the applied magnetic field decreases. And above the transition temperature the change in MR is very small.

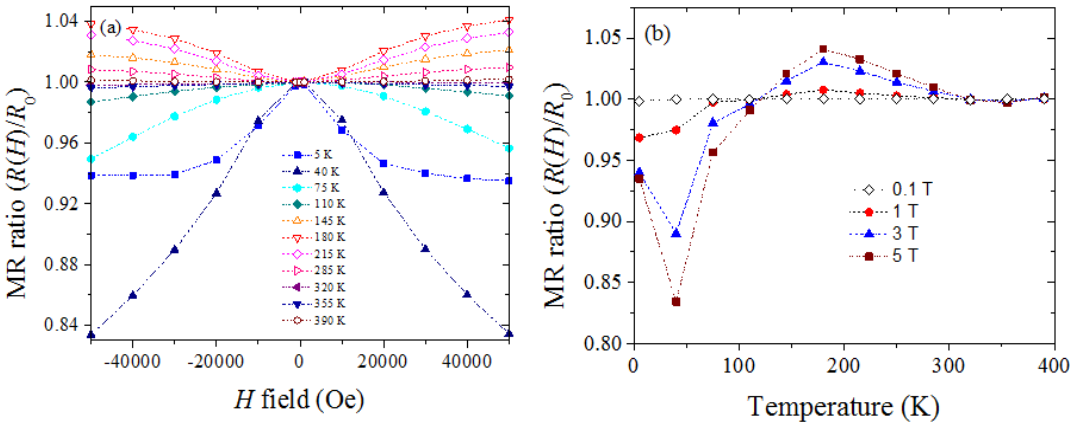

Fig. 6 (a) Magnetoresistance ratio ($R(H)/R(H=0)$) of the Mn_xGeAs_y film on Si(111) at various temperatures from 5 to 390 K.

Hall resistances with respect to temperature and external magnetic field have been measured. The anomalous Hall effect in a bar-patterned MnGeAs alloy film has been observed at low temperatures, less than 50 K, indicating the presence of spin polarized carriers. Above the temperature, anomalous Hall effect signal was not sufficient to be measured in the current measurement setup. At 355 K, above the transition temperature, the ordinary Hall effect was observed and the carriers have been determined n-type. A MnGeAs alloy film was deposited on an p-type GaAs(100) substrate and the current-voltage (*I-V*) characteristics measured, where a typical p-n diode type *I-V* curve was observed for the MnGeAs alloy film on a p-type GaAs, indicating that the MnGeAs alloy film layer is n-type.

IV. Conclusion

In conclusion, ZnMnGeAs alloy films have been synthesized on Si(100) and Si(111) substrates. The film samples have shown room-temperature ferromagnetisms observed and verified by temperature dependent electrical resistance and magnetization measurements including hysteric behavior at room temperature. Magnetoresistance measurements at various temperatures have displayed negative and positive MR values. The crossover happened between 110 and 145 K from negative to positive MR. ZnMnGeAs alloy films have n-type carriers and are potential candidates for room-temperature spintronic devices.

Acknowledgements

The present research has been conducted by the Research Grant of Kwangwoon University in 2015.

References

[1]. J. L. Shay and J. H. Wernick, *Ternary Chalcopyrite Semiconductors: Growth, Electronic Properties, and Applications*, (Pergamon Press, New York, 1975).
[2]. S. Cho, S. Choi, G.-B. Cha, S. C. Hong, Y. Kim, Y.-J. Zhao, A. J. Freeman, J. B. Ketterson, B. J. Kim, Y. C. Kim, B.-C. Choi, *Phys. Rev. Lett. 88* (2002) 257203.
[3]. G. A. Medvedkin, T. Ishibashi, T. Nishi, K. Hayata, Y. Hasegawa and K. Sato, *Jpn. J. Appl. Phys. 39* (2000) L949.
[4]. S. Cho *et al*., Phys. Rev B 66 (2002) 033303.
[5]. J. F. Gregg, in *Spin Electronics*, edited by Michael Ziese and Martin J. Thornton, (Springer 2001) pp.3-31.
[6]. G. A. Prinz, *Phys. Today 48(4)* (1995) 58.
[7]. S. Datta and B. Das, *Appl. Phys. Lett. 56* (1990) 665.
[8]. Y. Ohno, D. K. Young, B. Beschoten, F. Matsukura, H. Ohno and D. D. Awschalom, *Nature 402* (1999) 790.
[9]. R. Fiederling *et al., Nature 402* (1999) 787.
[10]. M. E. Overberg *et al*., *Appl. Phys. Lett. 79* (2001) 3128.
[11]. H. Ohno, A. Shen, F. Matsukura, A. Oiwa, A. Endo, S. Katsumoto and Y. Iye, *Appl. Phys. Lett. 69* (1996) 363.
[12]. X. Liu, Y. Sasaki, J. K. Furdyna, *Appl. Phys. Lett. 79* (2001) 2414.
[13]. D. Y. Park *et al*., *Science 295* (2002) 651.
[14]. S.Cho, S. Choi, G.-B. Cha, S. C. Hong, Y. Kim, A. J. Freeman, J. B. Ketterson, Y. Park and H.-M. Park, *Solid State Commun. 129* (2004) 609.
[15]. H. Li, Y. Xiao, B. Schmitz, J. Persson, W. Schmidt, P. Meuffels, G. Roth, T. Bruckel, *Sci. Rep. 2* (2012) 750.